

Thermal Behavior of Hollow and Solid Steel Beams with Different Boundary Conditions

Harbi A. DAUD¹⁾, Sultan A. DAUD²⁾, Adel A. AL-AZZAWI^{2)*}

¹⁾ *Institute of Technology
Middle Technical University
Baghdad, Iraq*

²⁾ *Civil Engineering Department
College of Engineering
Al-Nahrain University
Baghdad, Iraq*

*Corresponding Author e-mail: dr_adel_azzawi@yahoo.com

The thermal behavior of hollow steel structural members due to the temperature increase has not been investigated and discussed in many design codes. This work presents a study of the hollow and solid steel beams' carrying capacity under elevated temperatures. The material properties of such beams decline under the temperature expected to increase the moments on the beams. The finite difference technique is selected first to analyze the problem. The solved problems cover beams under concentrated point load levels with different end conditions such as cantilever, pin roller, and both ends fixed. The beam response (deflection, bending moment, and normal force) is examined. The finite element analysis was conducted using the DIANA FEA software to study the same problem incorporating material and geometric nonlinearities. It was found that both finite difference and finite element analysis solved the problem accurately when the temperature was under 500°C. It was also found that when the temperature was applied to the beam bottom face the deflection was smaller than when the temperature was applied to the side faces only and the whole section.

Keywords: hollow beams, finite difference analysis, finite element analysis, thermal loading, boundary conditions.

1. INTRODUCTION

Steel is a very strong construction material widely used in the construction of major structural elements. The use of steel as one of the most prevalent construction materials is due to its excellent mechanical properties such as higher ductility, higher modulus of elasticity, and higher tensile and compressive strength.

Its main drawbacks lower fire resistance resulting from its lower specific heat and higher thermal conductivity. The mechanical properties of steel decline with increasing temperature. Therefore, under fire conditions, steel structural members will have a diminished bearing load capacity due to the reduction in steel member strength and stiffness. In statically indeterminate structures, additional loads called thermal loading are applied to the structure along with the other gravity and horizontal wind and earthquake loads. The thermal loading results from the degradation of steel mechanical properties. The action of thermal loading due to the fire status may be considered as occasional action [1, 2]. Therefore, the design parameters for members in the case of fire should produce lesser magnitudes of effects than those for members at room temperature. The thermal loading in the case of fire is very important in controlling structural member safety. Many researchers have studied the response of steel structures exposed to thermal loading.

Usmani *et al.* acknowledged in 2001 that the analysis of fire-exposed composite steel-framed structures showed their greater resistance than in the standard testing of isolated elements in furnace. The study also showed that using design code equations is over-conservative and not based on logical methods. The most economical design of such structures to resist fire should be made after understanding the actual behavior of such members exposed to fire experimentally and theoretically [3].

In 2002, Wang proved that the change in the steel and concrete mechanical properties significantly affects the member response under fire as both materials have reduced properties and become weaker at increased temperature. The increase in temperature will produce an initial strain in the member. The study revealed that the response of such members could be fully understood if the material properties at higher temperatures were obtained accurately [4].

In 2007, Mourão *et al.* investigated the response of steel flexural members exposed to uniform temperature increase across the member section. The member was subjected to several uniform load levels. Also, the member had different end conditions (fixed-fixed, pinned-pinned, and pin-roller). Plots of deflection, normal force, bending moment and stresses, and variation with the temperature were given. The members were analyzed nonlinearly using finite elements ANSYS computer software. The steel stress-strain relationship variation with the temperature was used in the analysis [5].

A research work of Crosti in 2009 focused on studying the response of steel structures under thermal loading. The material was modeled as a thermoplastic one with geometric nonlinearities. A parametric curve for the response of steel members exposed to fire was used in the model. The study provided brief information on the preferred finite element codes used to model the problem properly. The strength and stiffness of each member were reduced with increasing tem-

perature. Besides, the assessment of the real building steel member or whole structure failure under the thermal loading is made [6].

Dwaikat and Kodur, in 2011, predicted the response of restrained steel flexural members or beams under fire. The finite element software ANSYS was used to carry out the analysis along with a theoretical one. The study tackled members with different end conditions, loading types, and thermal bowing effect [7].

Patade and Chakrabarti, in 2013, investigated the thermal stress and deformation responses of steel structures exposed to temperature increase. The increase in member temperature resulted in member expansion. For restrained end condition members, stresses developed, which affected the response of such structures. The axial force developed in the member due to fire accompanied by restrained end condition was very large and could result in unsafe design. The stiffness and strength of the member were reduced and this could lead to structural failure. In addition, the behavior of the steel flexural member subjected to ISO 834 fire standard with different end conditions was investigated [8].

Kucz *et al.*, in 2013, analyzed steel beams under fire with different end conditions. The beams were under uniformly distributed load and had restrained and unrestrained end conditions with a standard ISO-fire curve. The nonlinear thermal analysis was used to obtain the critical temperature. The ultimate limit state was evaluated at each temperature increment. During thermal expansion, an axial force developed for the restrained steel beams. The study numerical examples revealed that the member end conditions were predominant in investigating the actual response of such members in fire status. Also, the study showed that the member end conditions might affect the whole structure behavior and produce a lower critical temperature and time for fire resistance [9].

Patil and Ramgir, in 2016, carried out a thermal-structural analysis of steel flexural members under a concentrated load. The study comprised theoretical analysis for obtaining the deformation and stress of steel members with both ends fixed and single end fixed. Different cross-section sizes of members were used in the analysis. The restrained force developed in the fixed-ended beam was calculated and the resulting deformations and stresses were obtained. These developed forces are not recognized in the design of such members. The steel mechanical properties' reduction with temperature was also considered. The main objective of their work was to investigate the influence of increasing temperature on the deformation and stresses of steel members under point load. The finite elements ANSYS software analyzed the problem and compared the outcomes with experimental observations [10].

Lausova *et al.*, in 2016, carried out an analysis of steel members subjected to variable temperature distribution in the cross-section. The temperature increase produced additional internal forces in restrained ended members. The

beam section consisted of was non-protected hollow steel cross-sections of different sizes. The analysis was made using simplified calculations and finite element simulations of hollow steel members subjected to fire from three sides. The finite element analysis was verified with outcomes from the fire testing at the VSB-Technical University of Ostrava [11].

In the preceding literature, the details of investigating the mechanical properties of the solid section made from steel used in structural fire engineering were restricted to studies at ambient temperature. For the yield strength variation between peripheral and core material, the investigation showed high inhomogeneity, especially in the hot-rolled condition.

In 2017, Neuenschwander *et al.* published the results of a comprehensive series of tensile tests performed at variable temperatures ranging from 400 to 900°C under steady-state conditions. The ambient temperature variation between core and peripheral content coupon specimens for mild carbon steel was also investigated for different diameters of the solid section. The obtained temperature-dependent relations for the yield strength and ultimate tensile strength: (1) suggest only a minor difference between core and peripheral material, which for normalized small sections and hot-rolled thick sections disappears with increasing temperatures, and (2) can be reasonably forecasted by the European and North American design code models for structural steels at elevated temperature [12].

Łukomski *et al.*, in 2017, carried out an experimental fire resistance test of uncoated steel flexural members [13]. The outcomes were compared with simple and advanced calculation models given in EN 1993-1-2 [14]. The average difference between measured and calculated steel temperature was not more than 2%. All used approaches gave identical outcomes in terms of member collapse time. The approach used in Eurocode 3 [15] was found to be efficient in obtaining the fire resistance.

In 2017, Wong developed a numerical simulation to obtain the temperature variation of steel flexural elements exposed to fire. The previous methods assumed uniform sections under full fire status. In actual structures, the elements are often exposed to partial heating fire status. The elements may be exposed to multiple fire compartments or subjected to localized fires. Wong's study comprises a numerical study on the temperature variation of a partially heated steel beam using a finite difference method. The outcomes were compared with the available approaches given in Eurocodes. Therefore, the average temperature of a partially heated steel member was obtained. The proposed finite difference analysis results showed closer values to the real temperature distribution of steel members than the method given in Eurocodes [16].

This work aims to analyze numerically the behavior of statically determinate or indeterminate flexural members or beams under temperature increase and several loading levels. The finite difference and finite element techniques are

used to analyze the problem of hollow steel beams under thermal loading. The beams have different boundary conditions.

2. RESEARCH PROCEDURE

2.1. Finite difference study

The hollow or solid flexural member is modeled or simulated using finite differences by dividing it into equal-length segments (Δx) (Fig. 1). Here, the positioned node of the differential equation is called (i), and the total number of nodes is (n) in the finite difference expression. The deflected shape of the hollow or solid beam is simulated by a straight line connecting the nodes.

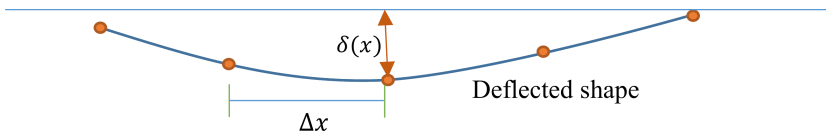


FIG. 1. Finite difference simulation.

The differential equations of deep flexural members derived in [17] are modified to include the thermal loadings as follows:

$$kG(T)A(T) \left(\frac{d\beta}{dx} + \frac{d^2\delta}{dx^2} \right) = q(x), \quad (1)$$

$$E(T)I(T) \frac{d^2\beta}{dx^2} - kG(T)A(T) \left(\beta + \frac{d\delta}{dx} \right) = \mu_T(x), \quad (2)$$

where $\delta = \delta(x)$ is the hollow or solid member deflection, $\beta = \beta(x)$ is the beam rotation, k is the shear correction factor, $G(T)$ is the shear modulus variation with temperature, $A(T)$ is the cross-sectional area variation with temperature, $E(T)$ is the modulus of elasticity variation with temperature, $I(T)$ is the moment of inertia of variation with temperature, $\mu_T(x)$ is the generated moments due to temperature variation (thermal bowing), and $q(x)$ is the distributed beam load.

For a rectangular section beam with breadth (b), depth (h), and length (L), after increasing temperature, the new dimensions become

$$b_{\text{new}} = b(1 + \alpha\Delta T), \quad h_{\text{new}} = h(1 + \alpha\Delta T), \quad L_{\text{new}} = L(1 + \alpha\Delta T), \quad (3)$$

where b_{new} , h_{new} and L_{new} are the breadth, depth, and length of the beam subjected to change in temperature, α is the coefficient of thermal expansion, and ΔT is the change in temperature.

The axial stress (σ_a) can be calculated theoretically using the following equation:

$$\sigma_a = E(T)\alpha \Delta T. \quad (4)$$

In actual cases of members subjected to elevated temperature, the temperature distribution in the structural element is usually not uniform, which results from the fact that there is the lower element face in contact with heat while the upper face is not. Therefore, the member top face will have a temperature much lower than that of its bottom face. Figure 2 shows the temperature variation in the flexural element heated from beneath. The temperature variation across the thickness of the flexural member is divided into two components. The first component is the uniform mean temperature increase (T_a), the second is the thermal bowing or temperature gradient (T_g), and their expressions are also shown in the figure.

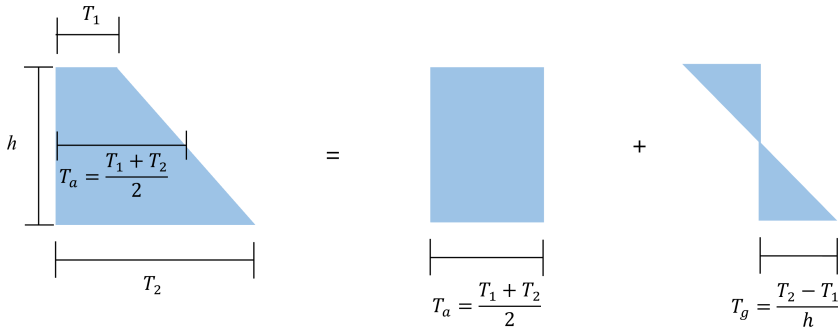


FIG. 2. Uniform average temperature and thermal gradient in the flexural member section.

The finite difference equations are written for an interior node (i) and the obtained simultaneous equations are solved to obtain the unknown displacements and, after that, the unknown stress resultants.

2.2. Finite element study

Usually, thermal analysis or heat transfer analysis is used to check the distribution of temperature at particular heat conditions on structural components. The thermal efficiency of the product can be improved by adjusting the location of the heat source, improving the methods of heat dissipation, applying thermal insulation, etc., once the thermal characteristics are determined from the simulation. The finite element method has become one of the most important methods for heat transfer analysis with the creation of computer-aided engineering (CAE). Like other forms of analysis, there are several nonlinear conditions in the heat transfer process. While it is possible to simplify certain procedures to linear problems, there are still many thermal nonlinearities that we need to consider

during the analysis. One of the most common nonlinearities in thermal problems is the temperature-dependent material properties, while the material properties exhibit nonlinearity in terms of temperature changes. Thermal conductivity, real heat, density, and enthalpy may be the nonlinear thermal material properties. Only the thermal conductivity parameter participates in the calculation in the steady-state analysis, while transient problems also need to consider real heat and mass density. Another nonlinearity is caused by boundary conditions that are dependent on temperature. In heat transfer analysis, the typical boundary conditions are temperature, heat flow, heat flux, convection, and radiation. Depending on the actual physical conditions, each of those boundary conditions may exhibit nonlinearity in terms of temperature changes. The DIANA FEA software was used in this paper to simulate experimental work done by Patil and Ramgir [10] and Crosti [6]. A 3D nonlinear finite element model was built to better understand the effect of increasing temperature on the deflection behavior of steel section beams shown in Fig. 3a. In the DIANA FEA program, structural

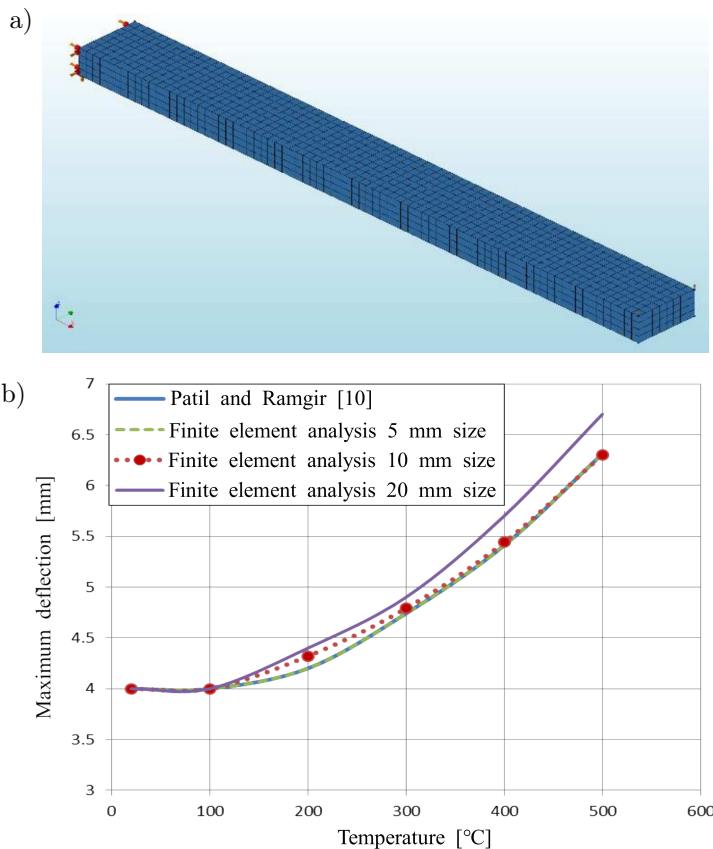


FIG. 3. Meshing: a) cantilever beam, b) verification.

and heat flow analyses were activated first. The thermal aspect of the material properties was defined in addition to von Mises' yield criteria based on the available data given in [19]. The accuracy of any finite element results is based on the selected mesh size of the problem [18]. So, the influence of mesh size must be carried out before starting model verification. To accomplish that, different mesh sizes with the same element type, boundary conditions, loading system, and thermal conditions and values were investigated. These different mesh sizes were used to simulate a cantilever beam loaded at the end and exposed to temperature variation. Three values were selected for the element size: 2.5, 5, and 8 mm. Figure 3b shows the simulation temperature-displacement curves compared with experimental results. The smallest error of these resultant errors was obtained with the element size 2.5 mm, as shown in the figure but with a higher solving time. Therefore, the element size of 5 mm provided a good accuracy for the present simulation, which is based on mesh sensitivity. The phased analysis was added to combine the transient heat transfer analysis with the structural nonlinear analysis.

3. RESULTS AND DISCUSSION

3.1. Verification

3.1.1. Cantilever beam. The problem of solid-section beam subjected to uniformly increasing temperature across its section, which was previously tested experimentally by Patil and Ramgir in [10], is selected in the present study for verification. The problem consists of a solid-section cantilever beam loaded with a concentrated load at the free end in addition to thermal loading, as shown in Fig. 4. The beam cross-section is solid and rectangular with breadth (b) equal to 40 mm and depth (h) of 20 mm. The beam has a length of 400 mm and is subjected to a concentrated load of 1000 N at the free end. The used material properties, given by Patil and Ramgir in [10], are in Table 1. Patil and Ramgir in [10] assumed the yield stress as constant with the variation of member temperature.

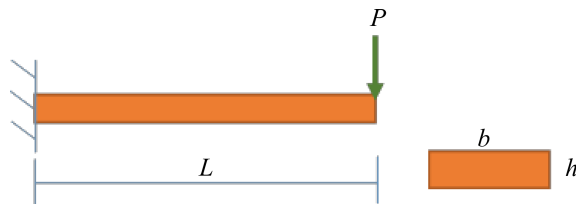


FIG. 4. The geometry and loading of cantilever beam with a solid cross-section.

TABLE 1. Material property for the beam [10].

Material property	Value				
Poisson's ratio [ν]	0.26				
Density (ρ) [kg/m^3]	7850				
Tensile strength [MPa]	400				
Yield stress [MPa]	250				
Coefficient of thermal expansion [$(\alpha)/^\circ\text{C}$]	12×10^{-6}				
Young's modulus [GPa]	200	189	168	147	126
Temperature [$^\circ\text{C}$]	20–100	200	300	400	500

Figure 5 shows the variation of maximum deflection at the free end with increasing temperature obtained from the experimental work of Patil and Ramgir [10] and the present study numerical solution. The obtained outcomes were too close to the experimental ones, with a maximum deviation of 5.6. Figure 6 also shows the variation of maximum bending stress with increasing temperature obtained from the same experimental work and the present study. The obtained finite element outcomes were too close to the experimental ones, with a maximum deviation of 2.7%. The finite-difference analysis shows a different trend to the experimental results. As the temperature increased, the bending stress decreased because, in finite differences, the analysis was assumed linear, while, in finite elements, the analysis was nonlinear.

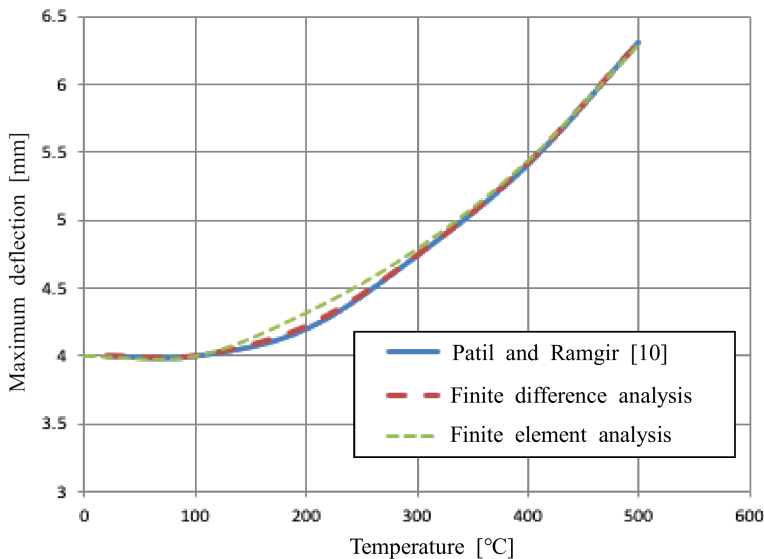


FIG. 5. Maximum deflection variation with temperature for the solid cantilever beam.

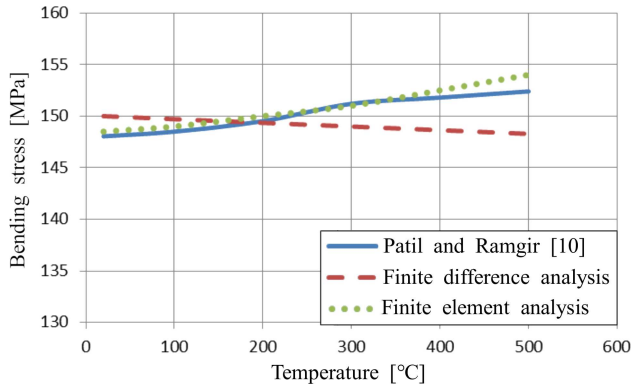


FIG. 6. Maximum bending stress variation with temperature for the solid cantilever beam.

3.1.2. Simply supported beam. The problem of solid-section beams subjected to uniform increasing temperature across their sections, previously suggested and analyzed using the finite element ADINA software by Crosti in [6], is selected in the present study for verification. The problem consists of simply supported (hinge-roller supports) solid-section beam loaded with a concentrated load at mid-span subjected in addition to thermal loading as shown in Fig. 7. The cross-section of the beam is square with a side length of 300 mm. The beam has a length of 3000 mm and is subjected to a concentrated load of 1410 kN at the free end for the cantilever beam and at the mid-span for the fixed-ended beam. The used Poisson's ratio (ν) is 0.26, density (ρ) is 7850 kg/m³, and other used material properties are given in Table 2.

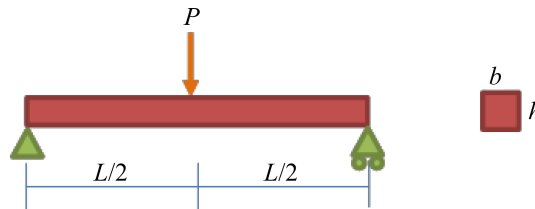


FIG. 7. The beam's geometry and loading.

TABLE 2. Material properties of the beam.

Yield stress [MPa]	Elastic Young's modulus [GPa]	After yield Young's modulus [GPa]	Coefficient of thermal expansion $[(\alpha)/^{\circ}\text{C}]$	Temperature [$^{\circ}\text{C}$]
235	210	10.5	12×10^{-6}	100
235	189	94.5	12.3×10^{-6}	200
235	168	84	12.6×10^{-6}	300
235	147	73.5	13×10^{-6}	400
183	126	63	13.1×10^{-6}	500

The problem is analyzed using finite differences, and its outcomes are shown together with the results of Crosti in Fig. 8. The obtained results show good agreement with the Crosti's results in terms of deflection with maximum differences of 1% in finite differences and 9% in finite elements.

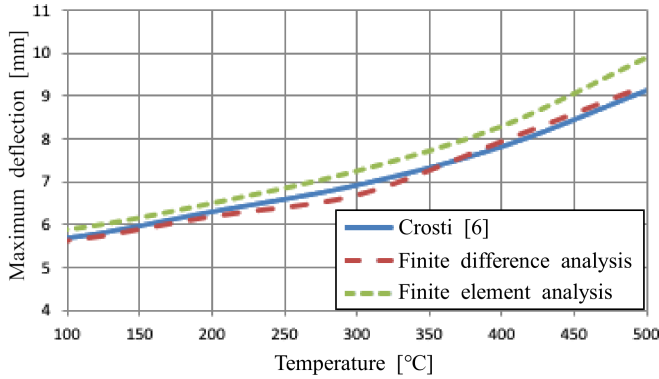


FIG. 8. Maximum deflection variation with temperature for the simply supported solid beam.

Patade and Chakrabarti [8] solved the same problem using finite element ABAQUS software assuming constant yield stress with temperature variation. Their results greatly differ from the results of Crosti, as shown in Table 3.

TABLE 3. Results of mid-span deflection for the two kinds of research.

Temperature [°C]	Deflection of mid-span [mm]	
	Patade and Chakrabarti [8]	Crosti [6]
100	20.5	5.6
200	22.7	6.13
300	25.6	6.65
400	29.3	7.83
500	34.2	9.24

3.2. Finite difference parametric study

A parametric study is carried out using finite differences for the same problems tested previously by Patil and Ramgir [10], assuming that the section is hollow with different thicknesses and end conditions, and considering uniform average temperature and thermal bowing effect, as shown in Fig. 9. An additional parametric study considering the effect of increasing beam depth, loading nature (uniform or concentrated) and coefficient of thermal expansion (constant or variable with temperature) were studied using finite elements.

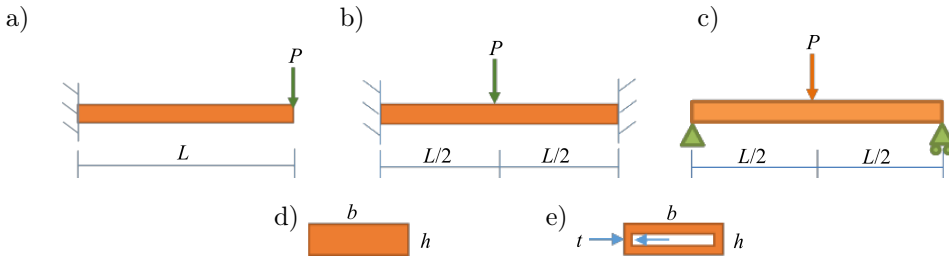


FIG. 9. The parametric study problem's geometry and loading: a) cantilever beam, b) fixed-ended beam, c) simply supported beam (present study), d) solid cross section [10], e) hollow cross-section (present study).

3.2.1. Section type (solid or hollow). Figure 10 shows the effect of changing hollow section thickness on the maximum deflection with different temperature increases for the cantilever beam with a hollow section. For 500°C, the maximum deflection increased by 56.6% with decreasing thickness from 6 mm to 2 mm. The effect of temperature increase on maximum deflection was lower for the 2 mm hollow section beam than for the others. Figure 11 shows that increasing hollow

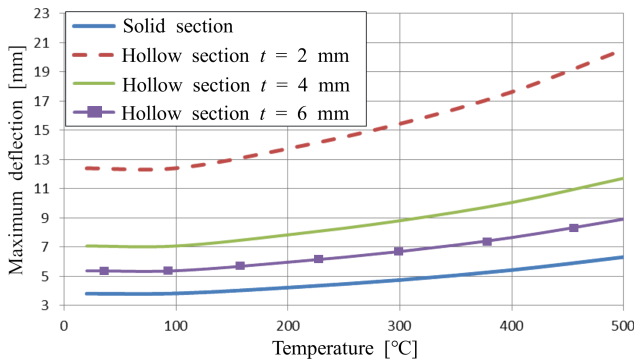


FIG. 10. The effect of temperature on the maximum deflection for the solid and hollow cantilever beam.

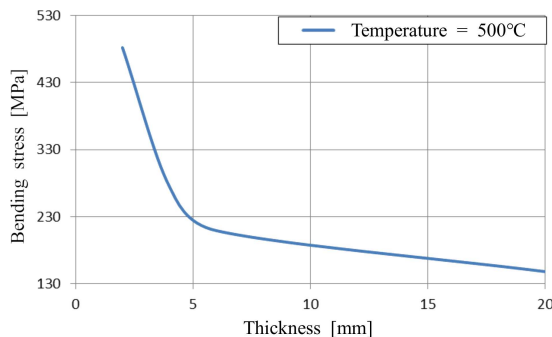


FIG. 11. The effect of section thickness on the bending stress for the hollow cantilever beam at a temperature of 500°C.

section thickness from 2 mm to 6 mm leads to a decrease in the bending stress by 69% because the section's moment of inertia increased due to temperature and thickness increase.

Figure 12 shows the effect of changing hollow section thickness on the maximum deflection with different temperature increases for the fixed-ended beam with a hollow section. For 20°C, the maximum deflection increased by 56.7% with decreasing thickness from 6 mm to 2 mm. For a temperature greater than 100°C, the increase in hollow section thickness has a reducing effect on the maximum deflection. The effect of temperature increase on the maximum deflection was smaller for the 2 mm hollow section beam than for the others. Figure 13 shows that increasing hollow section thickness from 2 mm to 6 mm leads to a decrease in the bending stress by 56.6% because of an increase in the section moment of inertia.

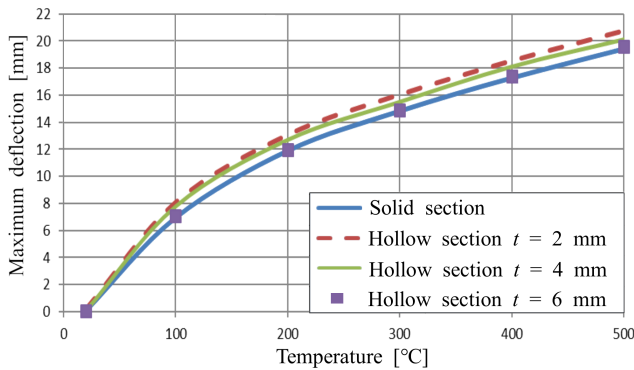


FIG. 12. The effect of temperature on the maximum deflection for the solid and hollow fixed-ended beam.

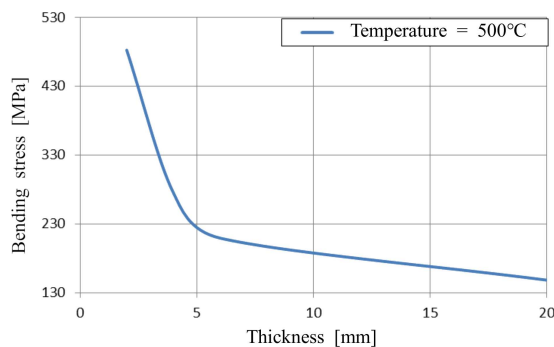


FIG. 13. The effect of section thickness on the bending stress for the hollow fixed-ended beam at a temperature of 500°C.

3.2.2. Boundary conditions. The effect of changing the end conditions for solid and hollow beams subjected to a uniform increase in temperature across

the section is shown in Figs 14 and 15. The fixed-ended beam shows a larger effect due to increasing temperature as a result of the developed restrained force that affects the stress and deflection in the beam regardless of the section type (solid or hollow).

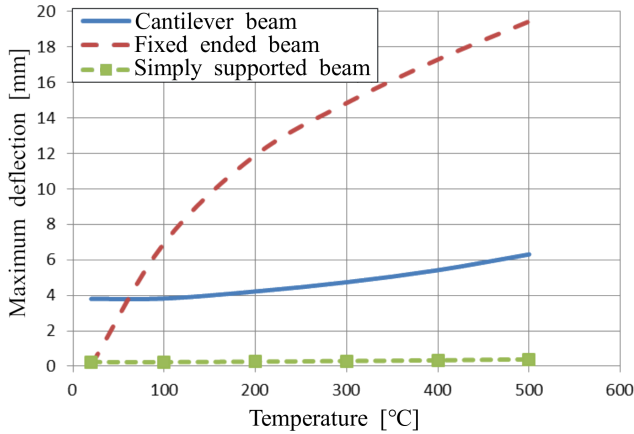


FIG. 14. The effect of temperature on the maximum deflection for the solid beam with different boundary conditions.

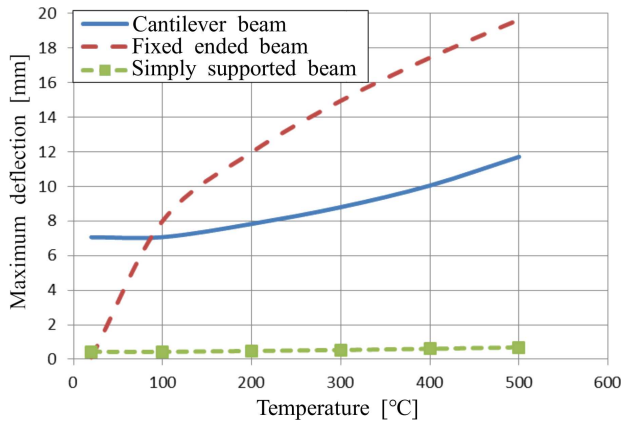


FIG. 15. The effect of temperature on the maximum deflection for the hollow beam (4 mm thickness) with different boundary conditions.

3.2.3. Thermal bowing. The effect of changing the temperature across the section of the simply supported beam (thermal bowing) for solid and hollow beams subjected to temperature variation across the beam section is shown in Figs 16 to 19. The thermal bowing affects the deflection of the beam by 200%, while the average uniform temperature increases affect the deflection by 65.6% regardless of the section type (solid or hollow). The thermal bowing affects the bending stress by 318% and 171% for solid and hollow beams, respectively. At

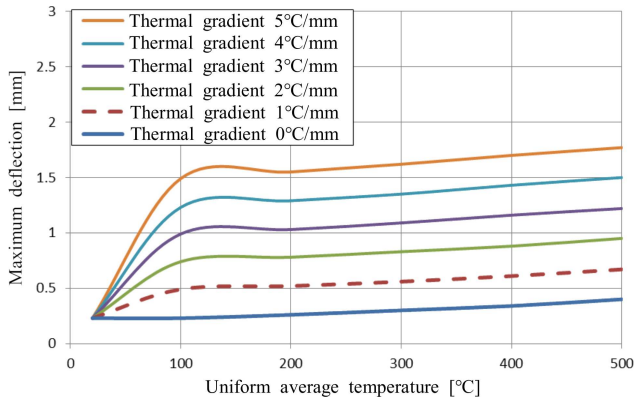


FIG. 16. The effect of thermal gradient on the maximum deflection for the solid beam with simply supported boundary condition.

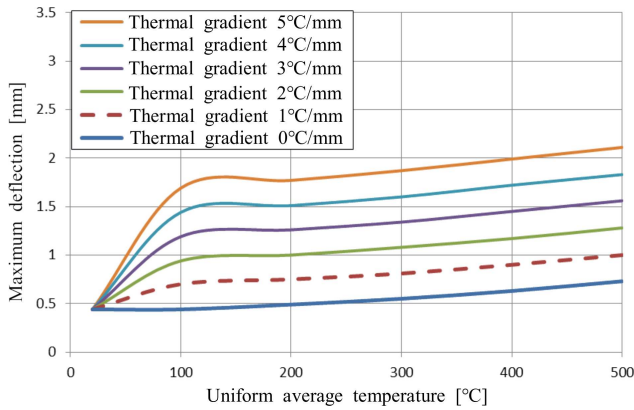


FIG. 17. The Effect of thermal gradient on the maximum deflection for the hollow beam (4 mm thickness) with simply supported boundary condition.

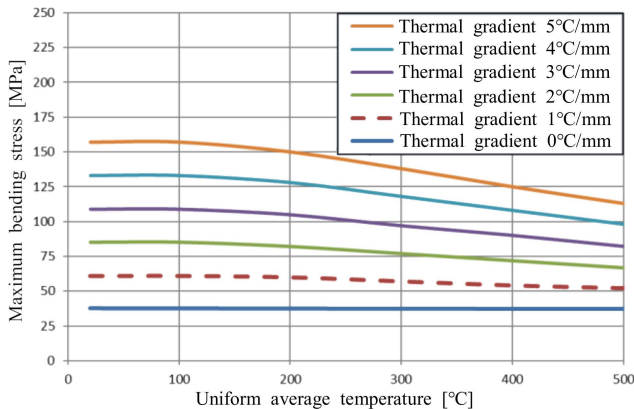


FIG. 18. The effect of thermal gradient on the maximum bending stress for the solid beam with simply supported boundary condition.

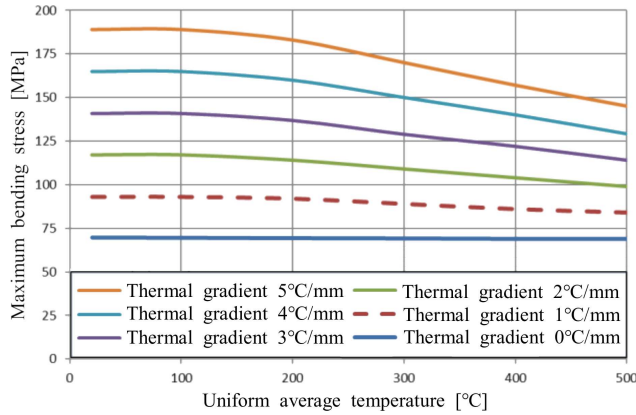


FIG. 19. The effect of thermal gradient on the maximum deflection for the hollow beam (4 mm thickness) with simply supported boundary condition.

the same time, the average uniform temperature increases affect the deflection by 28% for the thermal gradient of 5°C/mm regardless of the section type (solid or hollow).

3.3. Finite element parametric study

In this paper, the nonlinear finite element parametric study was carried out on a cantilever beam section with the same material proprieties and geometry as those presented by Patil and Ramgir [10]. The first parameters considered were cooling pipe effects, i.e., type of colling fluid (air or water) and the number of colling pipes. In Figs 20 and 21, it can be seen that the free end deflection was affected by the number of colling pipers, i.e., the deflection decreased with the increase in the number of colling pipes. Additionally, it was more effective

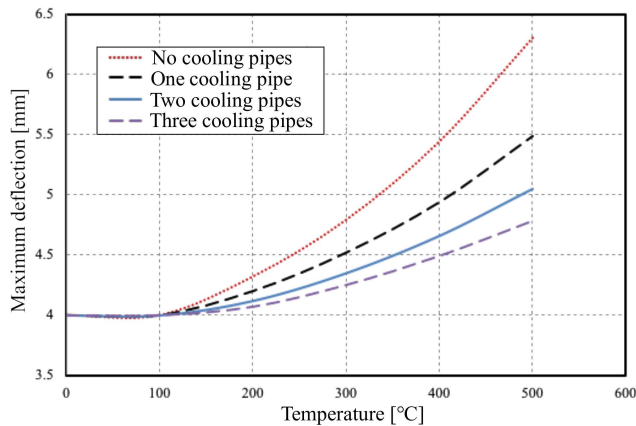


FIG. 20. The effect of thermal gradient on the maximum deflection for the solid beam with simply supported boundary condition.

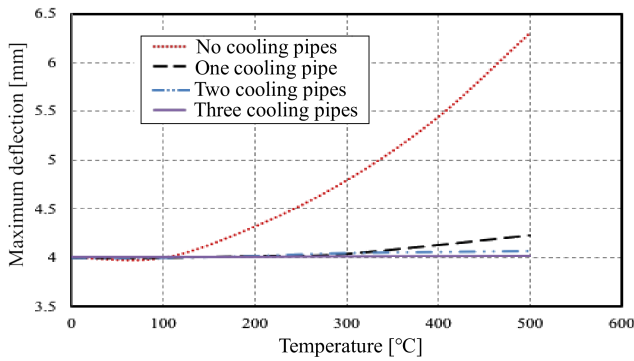


FIG. 21. The effect of thermal gradient on the maximum deflection for the hollow beam (4 mm thickness) with simply supported boundary condition.

for the case of air than the water cooling fluid. However, the free end deflection was reduced dramatically for the case of water (30% less), as shown in Fig. 22.

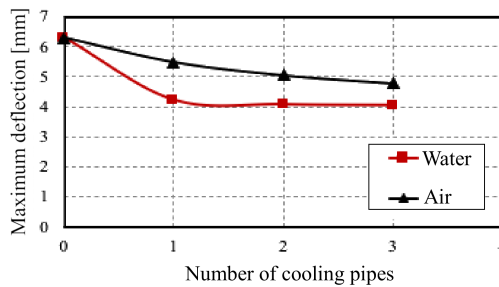


FIG. 22. The effect of thermal gradient on the maximum deflection for the hollow beam (4 mm thickness) with simply supported boundary condition.

The second parameter considered in this section was thermal bowing (temperature applied only to the bottom face, side faces, and whole faces) for two sections (solid and hollow). Firstly, it can be seen that the deflection of the hollow beams is bigger than that of solid beams for all cases (54%, 26%, and 62% for whole faces, side face only, and bottom face only, respectively), as shown in Figs 23 and 24. It can be also seen that the deflection is smaller when the temperature is applied to the bottom face than when the temperature is applied to the side faces only and the whole section. This is because, in the case of cantilever beams, the compression zone is at the bottom and when the temperature increases, the elastic modulus and other proprieties decrease. This leads to thermal stresses in the opposite direction to the bending stresses, i.e., negative bending (see Fig. 25), and it is more effective in the case of the solid section than the hollow section.

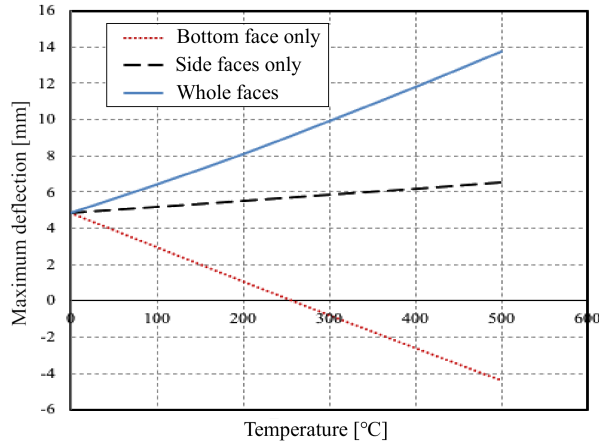


FIG. 23. The effect of thermal gradient on the maximum deflection for the solid beam with simply supported boundary condition.

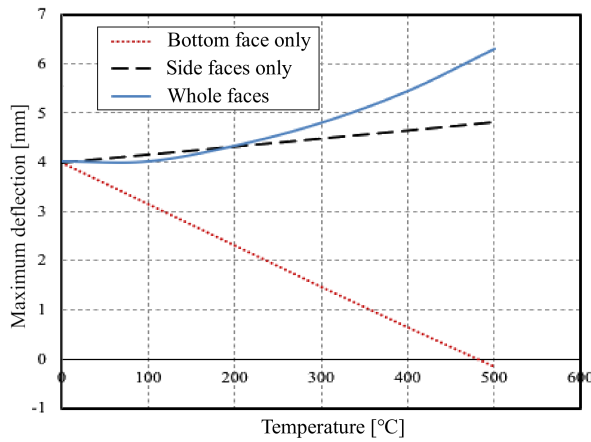


FIG. 24. The effect of thermal gradient on the maximum deflection for the hollow beam (4 mm thickness) with simply supported boundary condition.

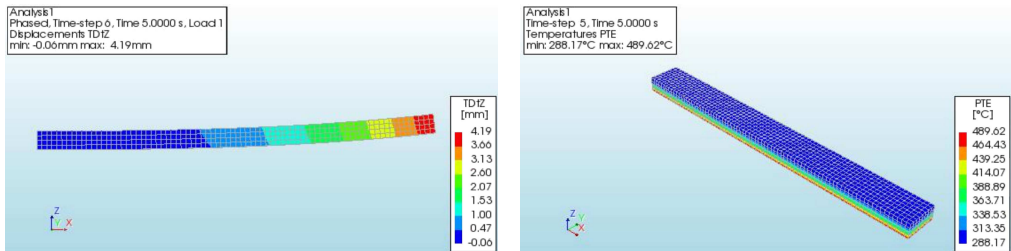


FIG. 25. a) Deflection shape of cantilever beam when the temperature applied to the bottom face; b) temperature gradients across the section.

4. CONCLUSION

The thermal load effect on the behavior of structural members due to the temperature increase has not been considered in many design codes. Therefore, the behavior of structural members with realistic boundary conditions at high temperatures must be investigated to obtain a solution with minimum cost and maximum safety. This work studied carrying capacity of the solid and hollow beams subjected to elevated temperature (up to $500^{\circ}\text{C}/\text{mm}$). The following conclusions can be drawn:

- For the solid cantilever beam, it is evident that the obtained outcomes were too close to the experimental results of previous research, with a maximum deviation of 5.6% for deflection and a maximum deviation of 2.7% for bending stress. For the simply supported beam, the obtained finite differences and finite elements results show good agreement with the results of Crosti [6] in terms of deflection with maximum differences of 1% and 9%, respectively.
- The effect of changing hollow section thickness on the maximum deflection with different temperature increase was investigated for the cantilever beam with a hollow section. For 500°C , the maximum deflection increased by 56.6% with thickness decreasing from 6 mm to 2 mm. The effect of temperature increase on the maximum deflection was lower for the 2 mm hollow section beam than for the others. It is obvious that increasing hollow section thickness from 2 mm to 6 mm leads to a decrease in the bending stress by 69% because the section's moment of inertia increased.
- The effect of changing the end conditions for solid and hollow beams subjected to a uniform increase in temperature across the section was studied. It is obvious that the fixed-ended beam showed a larger effect due to increasing temperature as a result of the developed restrained force that affects the stress and deflection in the beam regardless of the section type (solid or hollow). The effect of changing the temperature across the section of the simply supported beam (thermal bowing) for solid and hollow beams subjected to temperature variation across the beam section was investigated. It is obvious that the thermal bowing affects the deflection of the beam by 200%, while the average uniform temperature increases affect the deflection by 65.6% regardless of the section type (solid or hollow). The thermal bowing affects the bending stress by 318% and 171% for solid and hollow beams, respectively. At the same time, the average uniform temperature increases affect the deflection by 28% for the thermal gradient of $5^{\circ}\text{C}/\text{mm}$ regardless of the section type (solid or hollow).
- In finite elements, cooling pipe effects were studied. It is obvious that the free end deflection was affected by the number of cooling pipes, i.e., the de-

flection decreased with the increase in the number of cooling pipes. It was more effective for the case of air than the water cooling fluid. However, the free end deflection was reduced dramatically for the case of water (30% less). It is obvious from finite elements that the deflection of the hollow beams was bigger than that of solid beams for all cases (54%, 26%, and 62% for whole faces, side face only, and bottom face only, respectively). It can also be seen that the deflection was smaller when the temperature was applied to the bottom face than when the temperature was applied to the side faces only and the whole section.

ACKNOWLEDGEMENTS

We would like to thank Prof. John. P. Forth and Dr. Muhammed Kashif Shezad from the University of Leeds, UK for the software facilities.

REFERENCES

1. V.P. e Silva, R.H. Fakury, Brazilian standards for steel structures fire design, *Fire Safety Journal*, **37**(2): 217–227, 2002, doi: 10.1016/S0379-7112(01)00044-3.
2. Eurocode – Basis of structural design (EN 1990:2002+A1), European Committee for Standardization, Brussels, 2005.
3. A.S. Usmani, J.M. Rotter, S. Lamont, A.M. Sanad, M. Gillie, Fundamental principles of structural behavior under thermal effects, *Fire Safety Journal*, **36**(8): 721–744, 2001, doi: 10.1016/S0379-7112(01)00037-6.
4. Y.C. Wang, *Steel and Composite Structures Behavior and Design For Fire Safety*, Spon Press, London, New York, 2002.
5. H. dos R. Mourão, V.P. e Silva, On the behavior of single-span steel beams under uniform heating, *Journal of The Brazilian Society of Mechanical Sciences and Engineering*, **29**(1): 115–122, 2007, doi: 10.1590/S1678-58782007000100015.
6. C. Crosti, Structural analysis of steel structures under fire loading, *Acta Polytechnica*, **49**(1): 21–28, 2009, doi: 10.14311/1083.
7. M. Dwaikat, V. Kodur, Engineering approach for predicting fire response of restrained steel beams, *Journal of Engineering Mechanics*, **137**(7): 447–461, 2011, doi: 10.1061/(ASCE)EM.1943-7889.0000244.
8. H.K. Patade, M.A. Chakrabarti, Thermal stress analysis of beam subjected too fire, *International Journal of Engineering Research and Applications (IJERA)*, **3**(5): 420–424, 2013.
9. M. Kucz, K. Rzeszut, Ł. Polus, M. Malendowski, Influence of boundary conditions on the thermal response of selected steel members, *Procedia Engineering*, **57**: 977–985, 2013, doi: 10.1016/j.proeng.2013.04.124.
10. B.V. Patil, M.S. Ramgir, Study of structural steel members under thermal loading, *International Journal of Science, Engineering and Technology Research (IJSETR)*, **5**(8), 2016.

11. L. Lausova, I. Skotnicova, V. Michalcova, Thermal transient analysis of steel hollow sections exposed to fire, *Perspectives in Science*, **7**: 247–252, 2016, doi: 10.1016/j.pisc.2015.11.040.
12. M. Neuenschwander, M. Knobloch M. Fontana, Elevated temperature mechanical properties of solid section structural steel, *Construction and Building Materials*, **149**: 186–201, 2017, doi: 10.1016/j.conbuildmat.2017.05.124.
13. M. Łukomski, P. Turkowski, P. Roszkowski, B. Papis, Fire resistance of unprotected steel beams – comparison between fire tests and calculation models, *Procedia Engineering*, **172**: 665–672, 2017, doi: 10.1016/j.proeng.2017.02.078.
14. Eurocode 1: Actions on structures Part 1-2: General actions – Actions on structures exposed to fire (EN 1991-1-2), European Committee for Standardization, Brussels, 2002.
15. Eurocode 3: Design of steel structures-Structural fire design, prEN 1993-1-2, European Committee for Standardization, Brussels, 2003.
16. B. Wong, Temperature analysis of partially heated steel members in fire, *Journal of Constructional Steel Research*, **128**: 1–6, 2017, doi: 10.1016/j.jcsr.2016.08.008.
17. C. Chinwuba Ike, Timoshenko beam theory for the flexural analysis of moderately thick beams – variational formulation, and closed form solution, *TECNICA ITALIANA-Italian Journal of Engineering Science*, **63**(1): 34–45, 2019, doi: 10.18280/ti-ijes.630105.
18. M. Attaa, A.A. Abd-Elhady, A. Abu-Sinna, H.E.M. Sallam, Prediction of failure stages for double lap joints using finite element analysis and artificial neural networks, *Engineering Failure Analysis*, **97**: 242–257, 2019, doi: 10.1016/j.engfailanal.2019.01.042.
19. S.A. Daud, R.A. Daud, A.A. Al-Azzawi, Behavior of reinforced concrete solid and hollow beams that have additional reinforcement in the constant moment zone, *Ain Shams Engineering Journal*, **12**(1): 31–36, 2021, doi: 10.1016/j.asej.2020.07.017.

Received February 23, 2021; revised version June 30, 2021.